

Dark sectors with dynamical coupling

Weiqiang Yang,^{1,*} Olga Mena,^{2,†} Supriya Pan,^{3,‡} and Eleonora Di Valentino^{4,§}

¹*Department of Physics, Liaoning Normal University, Dalian, 116029, P. R. China*

²*IFIC, Universidad de Valencia-CSIC, 46071, Valencia, Spain*

³*Department of Mathematics, Presidency University, 86/1 College Street, Kolkata 700073, India*

⁴*Jodrell Bank Center for Astrophysics, School of Physics and Astronomy,
University of Manchester, Oxford Road, Manchester, M13 9PL, UK*

Coupled dark matter-dark energy scenarios are modeled via a dimensionless parameter ξ , which controls the strength of their interaction. While this coupling is commonly assumed to be constant, there is no underlying physical law or symmetry that forbids a time-dependent ξ parameter. The most general and complete interacting scenarios between the two dark sectors should therefore allow for such a possibility, and it is the main purpose of this study to constrain two possible and well-motivated coupled cosmologies by means of the most recent and accurate early and late-time universe observations. We find that CMB data alone prefers $\xi(z) > 0$ and therefore a smaller amount of dark matter, alleviating some crucial and well-known cosmological data tensions. An objective assessment of the Bayesian evidence for the coupled models explored here shows no particular preference for the presence of a dynamical dark sector coupling.

Keywords: Dark matter and dark energy, interacting cosmologies, cosmological observations

1. INTRODUCTION

Dark matter and dark energy, according to a series of observational evidences, are the two main constituents of the universe, comprising nearly 96% of its total energy density [1]. For the last twenty years, a huge observational effort has been devoted to unravel the nature of these two fluids [2, 3, 4, 5, 6]. Despite the fact that some of their properties have been measured with unprecedented accuracy (the value of the dark energy equation of state with 95% CL errors is $w = -1.028^{+0.063}_{-0.061}$ from the latest Cosmic Microwave Background (CMB) data, combined with large scale structure observations and Supernovae Ia luminosity distances [1]), their nature still remains obscure. Furthermore, the so-called *why now* problem provides another puzzle that may suggest a contemporary evolution of the two dark fluids. From the particle physics perspective, if a cosmic scalar field is responsible for the dark energy component, it may couple to all other fields in nature, if it is present [7]. These models emerged as coupled quintessence [8, 9, 10, 11, 12, 13]. Indeed, the presence of an interaction between the two dark fluids could successfully address the cosmic coincidence problem. Furthermore, some quintessence models could also be interpreted as modified gravity (Brans-Dicke-like) theories. An extra bonus supporting interactions among the two dark sectors arises from the fact that, when dark matter and dark energy interact, an effective equation of state $w < -1$ could naturally appear [14, 15, 16]. While plenty of work in the literature has been devoted to explore the rich phenomenology of

these models [17, 18, 19, 20, 21, 22, 23, 24, 25, 26, 27, 28, 29, 30, 31, 32, 33, 34, 35, 36, 37, 38, 39, 40, 41, 42, 43], more recently, an extra encouraging aspect of these theories has improved their role as an alternative to a pure Λ CDM universe. Namely, in dark matter-dark energy coupled cosmologies the tension between local and CMB estimations of the Hubble constant H_0 could be ameliorated [44, 45, 46, 47].

Current cosmological observations still allow for significant interactions among the two dark sectors, i.e. between dark matter and dark energy, see e.g. Refs. [48, 49, 50, 51, 52, 53]. In this work we consider an interacting scenario in which vacuum interacts with pressure-less dark matter adopting the more general phenomenological viewpoint, i.e. inspecting a time-dependent coupling. Such a consideration also entails the case of a coupling parameter that remains constant in cosmic time. For our analyses we have assumed that our universe is homogeneous and isotropic, that is, its geometry is well described by the Friedmann-Lemaître-Robertson-Walker line element.

The work has been organized as follows. Section 2 contains the gravitational equations within an interacting universe. In Sec. 3 we describe the observational data and the methodology used to constrain the interacting dark energy models. Section 4 presents the observational constraints on the models, including also a Bayesian evidence analysis. Finally, we draw our conclusions in Sec. 5.

2. GRAVITATIONAL EQUATIONS OF A UNIVERSE WITH INTERACTING DARK SECTORS

A homogeneous and isotropic universe is well described by the Friedmann-Lemaître-Robertson-Walker (FLRW) metric:

*Electronic address: d11102004@163.com

†Electronic address: omena@ific.uv.es

‡Electronic address: supriya.maths@presiuniv.ac.in

§Electronic address: eleonora.divalentino@manchester.ac.uk

$$ds^2 = -dt^2 + a^2(t) \left[\frac{dr^2}{1 - \kappa r^2} + r^2 (d\theta^2 + \sin^2 \theta d\phi^2) \right], \quad (1)$$

in which $a(t)$ is the expansion scale factor of the universe and $\kappa = 0, +1$, and -1 correspond to a spatially flat, closed and open universe, respectively. In the following, we shall assume that the gravitational sector of the theory is described by the Einstein gravity and $\kappa = 0$. Within this simple cosmological scenario, we will introduce an interaction between the pressure-less cold dark matter component and the dark energy fluid, acting as vacuum energy. All in all, the conservation equations read as

$$\nabla^\mu (T_{\mu\nu}^{\text{CDM}} + T_{\mu\nu}^{\text{DE}}) = 0, \quad (2)$$

where $T_{\mu\nu}^i$ ($i = \text{CDM, DE}$) is the energy-momentum tensor for the i -th dark sector. Considering the dark energy fluid as a cosmological constant with an equation of state $w_x = p_x/\rho_x = -1$, the conservation equations are given by

$$\dot{\rho}_x = Q, \quad (3)$$

$$\dot{\rho}_c = -3H\rho_c - Q, \quad (4)$$

where the dot refers to derivatives respect to the time t , $H \equiv \dot{a}/a$ is the Hubble parameter, ρ_c is the cold dark matter mass-energy density and Q encodes the interaction rate between the dark fluids. Our analyses will

be applied to two possible models, named as Interacting Vacuum Scenario 1 and 2 (IVS1 and IVS2, respectively):

$$\text{IVS1 : } Q = 3\xi(a)H\rho_x, \quad (5)$$

$$\text{IVS2 : } Q = 3\xi(a)H \frac{\rho_c \rho_x}{\rho_c + \rho_x}, \quad (6)$$

where $\xi(a)$ is a time-dependent dimensionless coupling. A Taylor expansion of $\xi(a)$ around the present time ($a = 1$) leads to

$$\xi(a) = \xi_0 + (a - 1)\xi'(a_0 = 1) + \frac{(a - 1)^2}{2!}\xi''(a_0 = 1) + \dots \quad (7)$$

where the prime stands for the derivative with respect to the scale factor. In this work, we shall restrict ourselves to linear corrections of $\xi(a)$. We therefore consider the following parameterization of the time dependent coupling parameter

$$\xi(a) = \xi_0 + \xi_a (1 - a), \quad (8)$$

where we use ξ_a instead of $\xi'(a_0 = 1)$. We note that the above choice was used recently by the authors of [54] and earlier in [59, 60].

For the first interaction model (IVS1) it is possible to obtain an analytical solution for the background evolution of the dark sector fluids:

$$\rho_x = \rho_{x0} a^{3(\xi_0 + \xi_a)} \exp(-3\xi_a(a - 1)), \quad (9)$$

$$\rho_c = \rho_{c0} a^{-3} - 3\rho_{x0} a^{-3} \int_1^a [\xi_0 + \xi_a(1 - a)] a^{3(\xi_0 + \xi_a) + 2} \exp(-3\xi_a(a - 1)) da. \quad (10)$$

For the IVS2 model the background evolution needs to be computed numerically.

To evaluate the perturbations equations in the presence of an interaction we work within the perturbed FLRW metric [55, 56, 57] and follow the synchronous gauge, see Ref. [58] for details.

Last but not least, we note that if in IVS1, the interaction function is simply considered as $Q = \Gamma\rho_x$, where Γ is purely a time-independent constant, that means if the interaction rate depends solely on the dark energy component not on other physical parameters, such as the Hubble expansion rate, scale factor of the universe, etc., it is then believed that such cosmological models should reflect more light on the intrinsic properties of the dark energy. Similarly, without assuming any interaction in the dark sector, one could also construct some physically motivated phenomenological dark energy models where

dark energy could decay with the evolution of the universe leading to a class of metastable dark energy models [61, 62, 63, 64].

3. OBSERVATIONAL DATA AND STATISTICAL METHOD

In this section we describe the cosmological observations that we have used to constrain the interacting scenarios. A discussion concerning the statistical method used in our analyses is also detailed. The publicly available datasets that we exploit in what follows are:

- **Cosmic Microwave Background (CMB):** We use the Cosmic Microwave Background measurements from Planck 2015 data release [65, 66], which include both the high- ℓ ($30 \leq \ell \leq 2508$) TT and the

low- ℓ ($2 \leq \ell \leq 29$) TT likelihoods. The Planck polarization likelihood in the low- ℓ multipole regime ($2 \leq \ell \leq 29$), together with the high-multipole ($30 \leq \ell \leq 1996$) EE and TE likelihoods are also considered. Despite the fact that all these likelihoods have a clear dependence on a given number of nuisance parameters, such as residual foreground contamination, calibration, and others, we have also accounted for those in our numerical analyses and marginalized over them when presenting the final constraints.

- **Baryon acoustic oscillation (BAO)** distance measurements: we use the BAO data from different observational missions, see Refs. [67, 68, 69].
- **Supernovae Type Ia (Pantheon)**: The Supernovae Type Ia (SNIa) were the first indicators for an accelerating phase of the universe. Here, we use the latest compilation of SNIa data (known as Pantheon sample) comprising 1048 data points [70].
- **Hubble constant (R19)**: Finally, we shall also consider the impact of a recent estimation of the Hubble constant, $H_0 = 74.03 \pm 1.42$ km/s/Mpc at 68% CL [71], which shows a high tension (4.4σ) with CMB estimates *within the minimal Λ CDM cosmological model*.

We however combine these datasets in the context of our IVS1 and IVS2 dark matter-dark energy models, see Eqs. (5) and (6), to explore whether this tension could be alleviated within these non-standard cosmologies.

For the statistical analyses, we make use of `cosmomc`, a Markov chain Monte Carlo package [72, 73], equipped with the Gelman and Rubin statistics for convergence diagnosis. This software also includes the support for the Planck 2015 likelihood [66]. The parameter space we shall constrain is

$$\mathcal{P} \equiv \left\{ \Omega_b h^2, \Omega_c h^2, 100\theta_{MC}, \tau, \xi_0, \xi_a, n_s, \log[10^{10} A_S] \right\}, \quad (11)$$

in which $\Omega_b h^2$ is the physical density for baryons; $\Omega_c h^2$ is the physical density for CDM; θ_{MC} denotes the ratio of sound horizon to the angular diameter distance; τ is the reionization optical depth; n_s denotes the scalar spectral index; A_S denotes the amplitude of the primordial scalar power spectrum and ξ_0, ξ_a control the interaction rate among the two dark sectors. We are therefore exploring an eight-dimensional parameter space with two extra degrees of freedom compared to the six-dimensional Λ CDM cosmology. We note that in the present work we are considering the spatially flat FLRW universe. Table I presents the priors imposed on the model parameters for the statistical analyses.

Parameter	Prior
$\Omega_b h^2$	[0.005, 0.1]
$\Omega_c h^2$	[0.01, 0.99]
τ	[0.01, 0.8]
n_s	[0.5, 1.5]
$\log[10^{10} A_S]$	[2.4, 4]
$100\theta_{MC}$	[0.5, 10]
ξ_0	[-1, 1]
ξ_a	[-1, 1]

TABLE I: Flat priors imposed on various cosmological parameters of the interacting dark energy scenarios.

4. NUMERICAL ANALYSES AND RESULTS

In this section we shall present the constraints on the interacting scenarios IVS1 and IVS2 (Eqs. (5) and (6) respectively), arising from the combination of several datasets, namely, CMB, CMB+R19, CMB+BAO, CMB+BAO+R19, and CMB+BAO+Pantheon.

4.1. IVS1: $Q = 3[\xi_0 + \xi_a(1 - a)]H\rho_x$

The observational constraints for this interacting dark energy scenario have been displayed in Table II. Figures 1 and 2 depict the one-dimensional marginalized posterior distributions and the two-dimensional joint contours for some selected cosmological parameters. Notice from Tab. II that the mean values of the parameters ξ_0 and ξ_a , quantifying the interaction among the dark sectors, are of opposite signs, and even if values $(\xi_0, \xi_a) \neq (0, 0)$ are still allowed by the observational data, a non-interacting scenario is consistent within 68% CL. Figures 1 and 2 show the strong anti-correlation between the interaction parameters ξ_0 and ξ_a .

Concerning the value of H_0 within the IVS1 interacting scheme, note that it is slightly larger than that obtained with Planck CMB data alone in the context of a Λ CDM model [6]. Due to the larger error bars on H_0 , the 4σ tension between local measurements (74.03 ± 1.42 km/s/Mpc [71]) and CMB observations is reduced to 2 standard deviations. Combining the CMB dataset with a gaussian prior on H_0 from R19, see the fifth column of Tab. II, we obtain $\xi_a = 0.55^{+0.50}_{-0.52}$ at 95% CL, i.e. different from zero with a significance of 2 standard deviations. The dynamical evolution of the coupling parameter $\xi(z)$ is illustrated on the left panel of Fig. 3 considering the CMB (solid curve) and the CMB+R19 data combination (dotted curve), where all the parameters have been fixed to their mean values. As for the CMB+R19 data combination the dynamical coupling $\xi(z)$ is larger than zero, the matter density shifts towards a lower value (see the strong anti-correlation between Ω_{m0} and ξ_0 in Fig. 1) and therefore there is not an increase in the quantity $S_8 \equiv \sigma_8 \sqrt{\Omega_{m0}/0.3}$. Consequently, in this case, the ten-

Parameters	CMB	CMB+BAO	CMB+BAO+Pantheon	CMB+R19	CMB+BAO+R19
$\Omega_c h^2$	$0.106^{+0.039}_{-0.040}$	$0.116^{+0.035}_{-0.044}$	$0.121^{+0.025}_{-0.023}$	$0.084^{+0.032}_{-0.026}$	$0.085^{+0.037}_{-0.030}$
$\Omega_b h^2$	$0.02220^{+0.00032}_{-0.00031}$	$0.02224^{+0.00031}_{-0.00029}$	$0.02226^{+0.00029}_{-0.00031}$	$0.02223^{+0.00031}_{-0.00028}$	$0.02223^{+0.00039}_{-0.00030}$
$100\theta_{MC}$	$1.0413^{+0.0027}_{-0.0025}$	$1.0408^{+0.0027}_{-0.0020}$	$1.0404^{+0.0014}_{-0.0015}$	$1.0426^{+0.0018}_{-0.0021}$	$1.0426^{+0.0019}_{-0.0023}$
τ	$0.079^{+0.035}_{-0.033}$	$0.082^{+0.035}_{-0.036}$	$0.083^{+0.036}_{-0.036}$	$0.077^{+0.045}_{-0.032}$	$0.078^{+0.035}_{-0.036}$
n_s	$0.9731^{+0.0088}_{-0.0084}$	$0.9747^{+0.0081}_{-0.0084}$	$0.9750^{+0.0085}_{-0.0084}$	$0.9740^{+0.0086}_{-0.0082}$	$0.9741^{+0.0090}_{-0.0090}$
$\ln(10^{10} A_S)$	$3.101^{+0.066}_{-0.065}$	$3.106^{+0.068}_{-0.070}$	$3.108^{+0.071}_{-0.071}$	$3.096^{+0.065}_{-0.062}$	$3.100^{+0.069}_{-0.069}$
ξ_0	$-0.01^{+0.21}_{-0.21}$	$-0.04^{+0.23}_{-0.20}$	$-0.04^{+0.15}_{-0.17}$	$-0.03^{+0.16}_{-0.17}$	$0.05^{+0.18}_{-0.21}$
ξ_a	$0.20^{+0.71}_{-0.56}$	$0.18^{+0.50}_{-0.46}$	$0.14^{+0.45}_{-0.37}$	$0.55^{+0.50}_{-0.52}$	$0.19^{+0.52}_{-0.48}$
Ω_{m0}	$0.27^{+0.13}_{-0.12}$	$0.30^{+0.09}_{-0.11}$	$0.313^{+0.062}_{-0.058}$	$0.202^{+0.067}_{-0.054}$	$0.214^{+0.082}_{-0.066}$
σ_8	$0.94^{+0.35}_{-0.28}$	$0.87^{+0.34}_{-0.22}$	$0.82^{+0.14}_{-0.14}$	$1.09^{+0.25}_{-0.27}$	$1.10^{+0.28}_{-0.32}$
H_0	$69.2^{+5.0}_{-5.0}$	$68.5^{+2.6}_{-2.4}$	$68.0^{+1.6}_{-1.6}$	$72.9^{+2.3}_{-2.4}$	$71.1^{+2.3}_{-1.9}$
S_8	$0.86^{+0.13}_{-0.09}$	$0.84^{+0.14}_{-0.07}$	$0.827^{+0.065}_{-0.060}$	$0.89^{+0.10}_{-0.11}$	$0.91^{+0.09}_{-0.11}$

TABLE II: Mean values and 95% CL errors on the cosmological parameters for the IVS1 interacting scenario, $Q = 3[\xi_0 + \xi_a(1-a)]H\rho_x$, using different combinations of the cosmological datasets considered here.

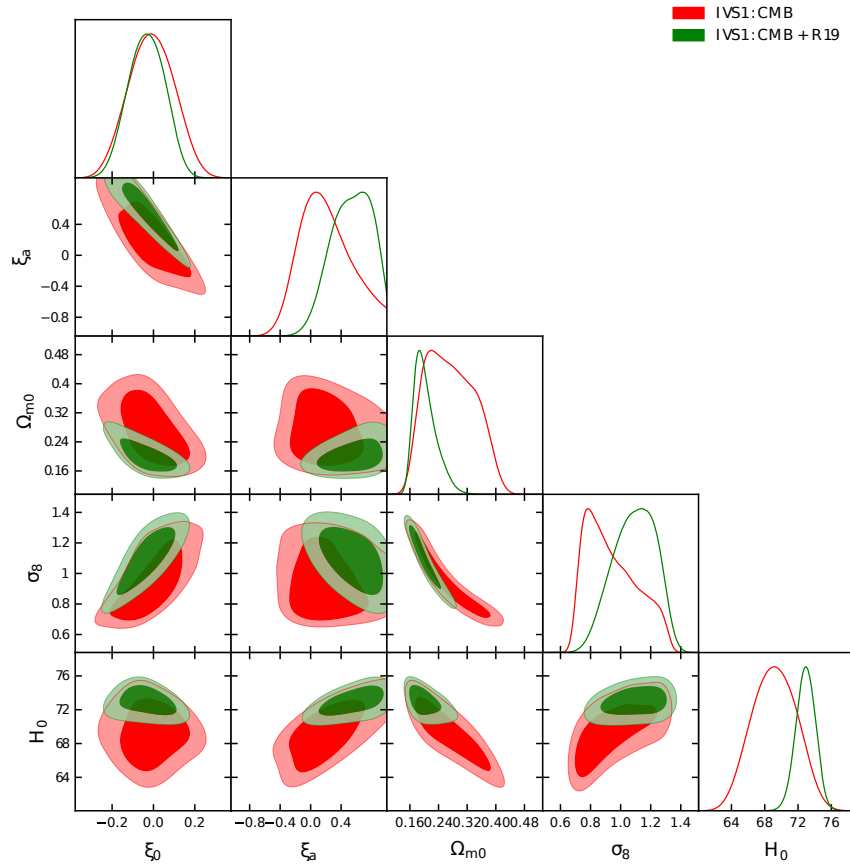


FIG. 1: Two-dimensional contours and one-dimensional marginalized posterior distributions for some key parameters of the IVS1 scenario for the CMB and CMB+R19 data sets.

sion at more than 2σ on S_8 [74] between Planck and the cosmic shear experiments, namely, KiDS-450 [75, 76, 77], DES [78, 79], and CFHTLenS [80, 81, 82] is solved within one standard deviation.

When adding the BAO dataset the error bars on the Hubble constant are notably decreased with respect to

what we observed with the CMB alone ¹. In this case the tension with R19 is only mildly alleviated, as it remains present at the 3σ level. The addition of BAO measure-

¹ The inclusion of BAO data to other datasets has a notable effect on the error bars on H_0 , see for instance [42, 83, 84].

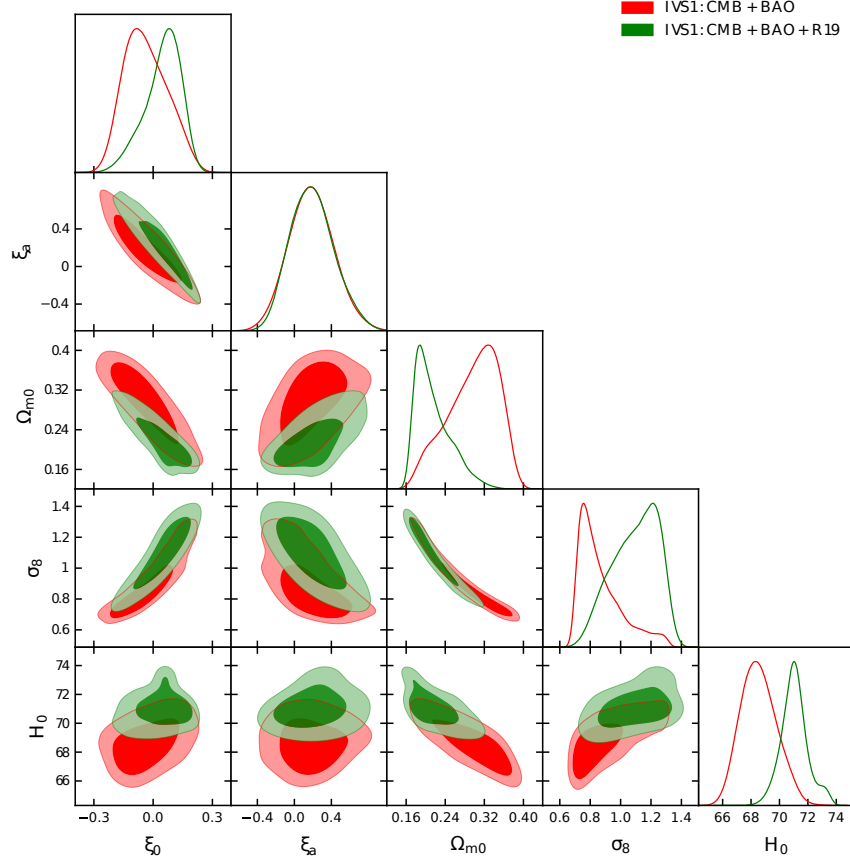


FIG. 2: Two-dimensional contours and one-dimensional marginalized posterior distributions for some key parameters of the IVS1 scenario for the CMB+BAO and CMB+BAO+R19 data sets.

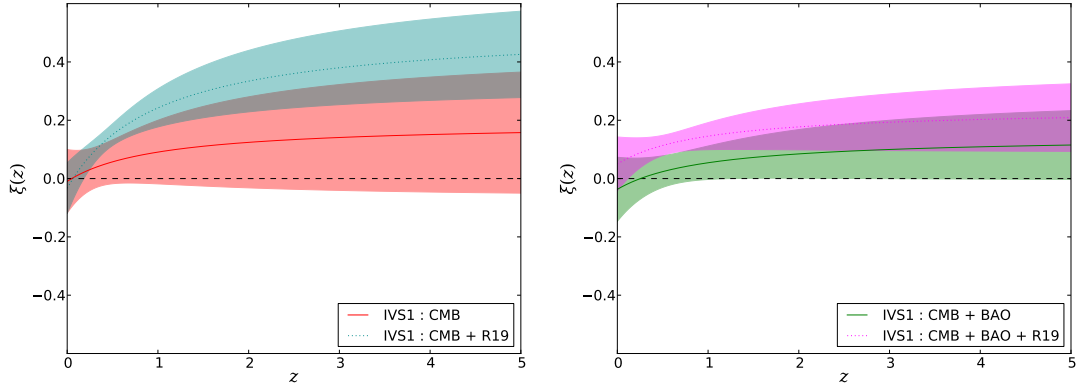


FIG. 3: Redshift evolution of the dynamical coupling parameter $\xi(z)$ ($1+z = a^{-1}$) for the IVS1 scenario using various observational datasets. The left panel corresponds to the CMB and CMB+R19 datasets while the right panel stands for the CMB+BAO and CMB+BAO+R19.

ments bring very close to zero the dynamical evolution of the dark sector coupling, see the right panel of Fig. 3.

Finally, when adding the Pantheon dataset to CMB+BAO (i.e. the combination named as CMB+BAO+Pantheon in Tab. II), we note that the estimation of H_0 shifts down and its error bars

are reduced, increasing therefore the tension with R19 measurements.

Parameters	CMB	CMB+BAO	CMB+BAO+Pantheon	CMB+R19	CMB+BAO+R19
$\Omega_c h^2$	$0.114^{+0.043}_{-0.048}$	$0.125^{+0.031}_{-0.036}$	$0.120^{+0.031}_{-0.032}$	$0.081^{+0.022}_{-0.019}$	$0.093^{+0.026}_{-0.022}$
$\Omega_b h^2$	$0.02219^{+0.00031}_{-0.00030}$	$0.02225^{+0.00029}_{-0.00030}$	$0.02226^{+0.00030}_{-0.00030}$	$0.02223^{+0.00030}_{-0.00028}$	$0.02220^{+0.00028}_{-0.00030}$
$100\theta_{MC}$	$1.0408^{+0.0027}_{-0.0025}$	$1.0402^{+0.0020}_{-0.0018}$	$1.0405^{+0.0017}_{-0.0016}$	$1.0428^{+0.0013}_{-0.0020}$	$1.0420^{+0.0015}_{-0.0016}$
τ	$0.080^{+0.034}_{-0.034}$	$0.083^{+0.034}_{-0.034}$	$0.084^{+0.033}_{-0.034}$	$0.086^{+0.030}_{-0.032}$	$0.080^{+0.037}_{-0.037}$
n_s	$0.9733^{+0.0095}_{-0.0085}$	$0.9749^{+0.0087}_{-0.0088}$	$0.9755^{+0.0081}_{-0.0078}$	$0.9751^{+0.0081}_{-0.0082}$	$0.972^{+0.011}_{-0.010}$
$\ln(10^{10} A_S)$	$3.105^{+0.066}_{-0.067}$	$3.108^{+0.066}_{-0.066}$	$3.109^{+0.064}_{-0.066}$	$3.114^{+0.066}_{-0.067}$	$3.106^{+0.073}_{-0.072}$
ξ_0	$-0.02^{+0.43}_{-0.38}$	$-0.17^{+0.41}_{-0.38}$	$-0.06^{+0.36}_{-0.40}$	$0.15^{+0.32}_{-0.30}$	$0.07^{+0.40}_{-0.37}$
ξ_a	$0.22^{+0.78}_{-0.59}$	$0.41^{+0.59}_{-0.59}$	$0.17^{+0.83}_{-0.45}$	$0.39^{+0.69}_{-0.74}$	$0.37^{+0.81}_{-0.87}$
Ω_{m0}	$0.30^{+0.15}_{-0.15}$	$0.321^{+0.094}_{-0.098}$	$0.312^{+0.077}_{-0.097}$	$0.195^{+0.053}_{-0.044}$	$0.229^{+0.062}_{-0.052}$
σ_8	$0.86^{+0.19}_{-0.17}$	$0.82^{+0.12}_{-0.11}$	$0.83^{+0.12}_{-0.10}$	$0.997^{+0.083}_{-0.088}$	$0.95^{+0.09}_{-0.10}$
H_0	$68.3^{+6.0}_{-6.2}$	$68.0^{+2.9}_{-2.6}$	$67.9^{+2.6}_{-2.2}$	$73.1^{+2.3}_{-2.4}$	$71.3^{+2.2}_{-2.2}$
S_8	$0.846^{+0.046}_{-0.068}$	$0.845^{+0.035}_{-0.039}$	$0.840^{+0.034}_{-0.039}$	$0.800^{+0.050}_{-0.047}$	$0.826^{+0.041}_{-0.042}$

TABLE III: Mean values and 95% CL errors on the cosmological parameters of the IVS2 interacting scenario, $Q = 3[\xi_0 + \xi_a(1-a)]H\frac{\rho_c\rho_x}{\rho_c+\rho_x}$, using different combinations of the cosmological datasets considered here.

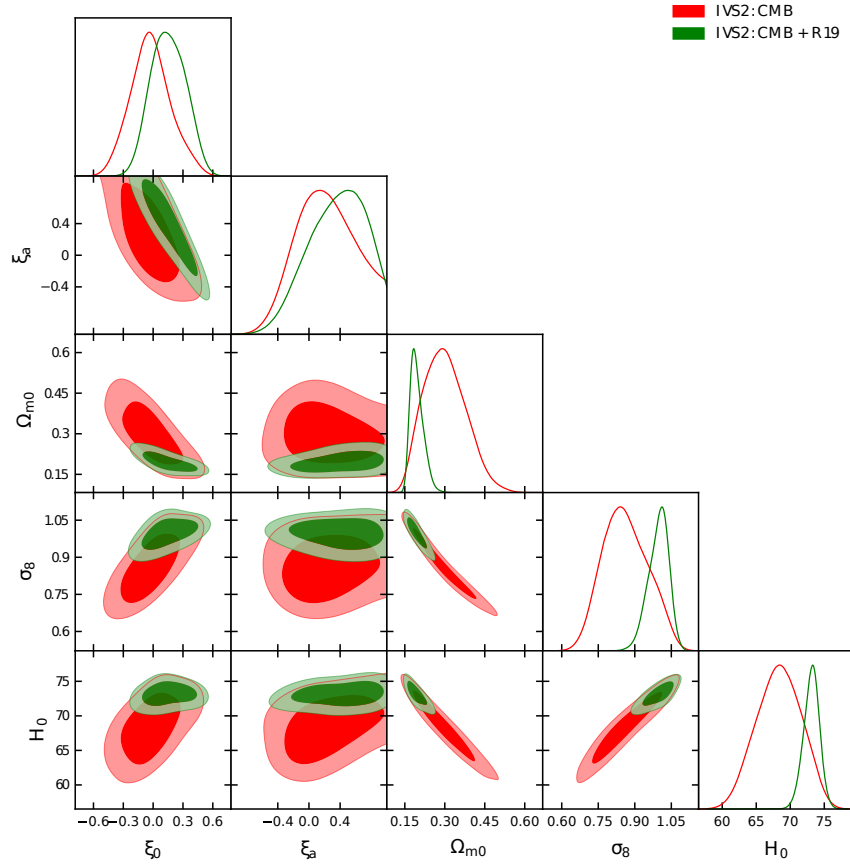


FIG. 4: Two-dimensional contours and one-dimensional marginalized posterior distributions for some key parameters of the IVS2 scenario for the CMB and CMB+R19 data sets.

4.2. IVS2: $Q = 3[\xi_0 + \xi_a(1-a)]H\frac{\rho_c\rho_x}{\rho_c+\rho_x}$

The summary of the observational constraints on this interaction scenario is shown in Tab. III, while in Figs. 4 and 5 we depict the one-dimensional marginalized posterior distributions and the two-dimensional contour plots for a number of both independent and derived cosmolog-

ical parameters, emphasizing their correlations with ξ_0 and ξ_a . Note that for CMB alone data the mean value of ξ_0 is almost zero with a very mild preference for negative values, while the mean value of ξ_a is found to be positive. When external datasets such as BAO or BAO plus Pantheon are added to CMB observations the tendency of ξ_0 (ξ_a) to take negative (positive) values is enhanced, show-

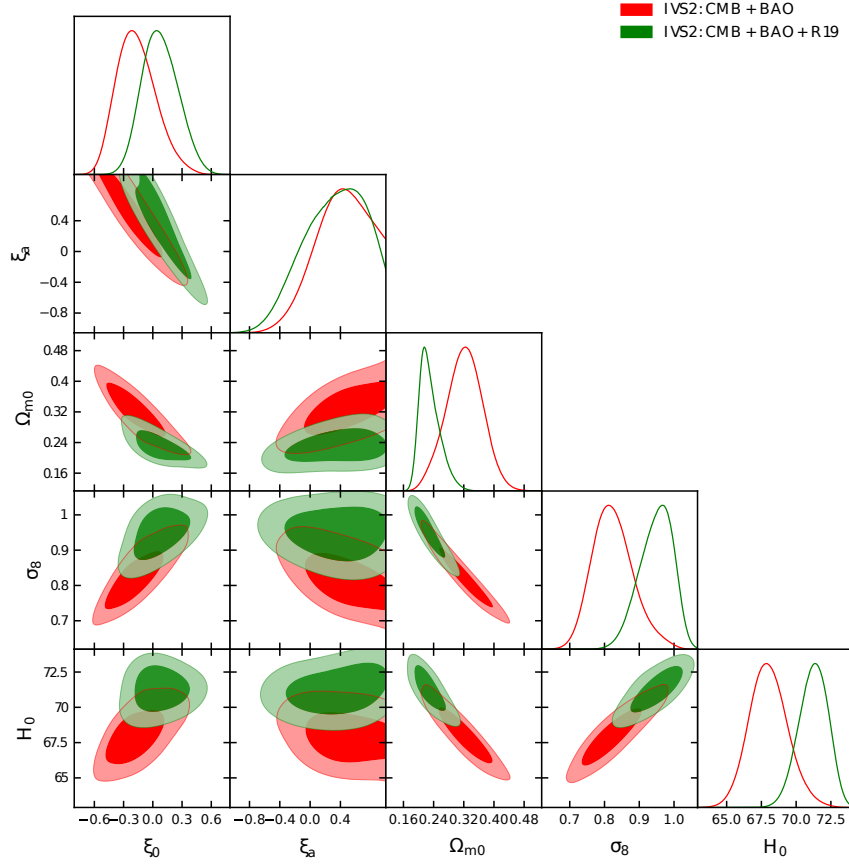


FIG. 5: Two-dimensional contours and one-dimensional marginalized posterior distributions for some key parameters of the IVS2 scenario for the CMB+BAO and CMB+BAO+R19 data sets.

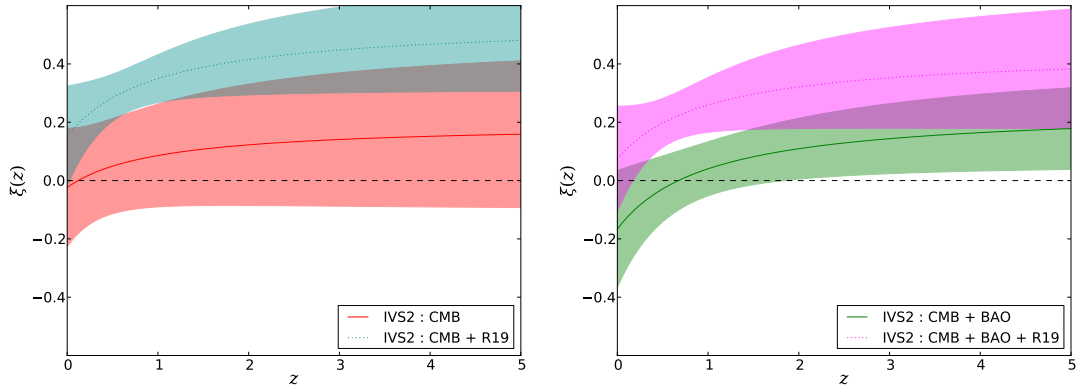


FIG. 6: We show the qualitative evolution of the dynamical coupling parameter $\xi(z)$ ($1+z=a^{-1}$) for the IVS2 scenario using various observational datasets. The left panel corresponds to the CMB and CMB+R19 datasets while the right panel stands for the CMB+BAO and CMB+BAO+R19.

ing opposite behaviors and a strong negative correlation between them, as we can see from Figs. 4 and 5 regardless of the observations considered in the analysis. Furthermore, from Tab. III, it is also possible to notice that for all the observational datasets the values $(\xi_0, \xi_a) = (0, 0)$ are allowed within 95% CL implying that we recover the

non-interacting Λ CDM limit. Nevertheless the dynamical interacting scenario cannot be ruled out and indeed, based on present observations, no definite conclusion can be made.

Focusing on the estimation of H_0 for this interaction scenario with CMB data only (see Tab. III), we notice

Dataset	Model	$\ln B_{ij}$
CMB	IVS1	5.9
CMB+BAO	IVS1	8.5
CMB+BAO+Pantheon	IVS1	4.1
CMB+R19	IVS1	2.8
CMB+BAO+R19	IVS1	9.9
CMB	IVS2	5.1
CMB+BAO	IVS2	7.7
CMB+BAO+Pantheon	IVS2	3.8
CMB+R19	IVS2	3.3
CMB+BAO+R19	IVS2	10.1

TABLE IV: The table summarizes the values of $\ln B_{ij}$ computed for the Λ CDM model with respect to the IVS models.

that it is slightly larger than within the Λ CDM scenario, and its error bars are increased due to the presence of a dynamical coupling. Due to the larger error bars on H_0 , for this model it is also possible to solve the tension with the local measurements of R19 [71]. Combining the CMB dataset with a gaussian prior on H_0 from R19 provides therefore a possible solution of both the Hubble constant tension and the S_8 tension with the cosmic shear data. The dynamical evolution of the coupling parameter $\xi(z)$ for this combination of data is shown in Fig. 6, notice that in this case there is also a tendency for $\xi(z) > 0$ for CMB + R19 and the addition of BAO data is less able to restore $\xi(z) = 0$ than within the IVS1 scenario. For CMB+BAO or CMB+BAO+Pantheon the situation is very similar to the dynamical IVS1 scenario aforementioned, i.e. neither the H_0 nor the S_8 tension are alleviated.

Finally, we comment on the results from a Bayesian evidence analysis of the dynamical interacting scenarios here explored. In this framework, a comparison of a cosmological model is performed with respect to a standard and well-motivated cosmological model [84, 85, 86, 87]. The Λ CDM provides the ideal choice for such a comparison. We can introduce the so-called Jeffreys scale, which, for different possible values of $\ln B_{ij}$, quantifies the strength of evidence of the reference, the canonical Λ CDM scenario (M_i), with respect to the underlying cosmological model (M_j) [88]. We have for $0 \leq \ln B_{ij} < 1$, a weak evidence; for $1 \leq \ln B_{ij} < 3$, a Definite/Positive evidence; for $3 \leq \ln B_{ij} < 5$, a strong evidence; and for $\ln B_{ij} \geq 5$, a very strong evidence for the Λ CDM model against the underlying cosmological scenario, here the interacting scenario. Following [85, 86] we compute the values of $\ln B_{ij}$ for all the observational datasets employed in this work, and present the results in Tab. IV. From this table, we learn that the Λ CDM model is always preferred over the two IVS models analyzed here. This is not surprising because Λ CDM has six free parameters while the two IVS models (IVS1 and IVS2) have eight free parameters. This fact eventually favors the base Λ CDM cosmology over the IVS models.

5. SUMMARY AND CONCLUSIONS

Non canonical cosmologies with an interaction between the dark matter and dark energy fluids have been widely investigated in the past several years. From the observational perspective, interacting theories have been found to provide a very promising way to solve the tension between early and late universe cosmological estimates of the Hubble constant. The present work generalizes interacting dark matter-dark energy models by considering a dynamical, redshift-dependent, coupling parameter.

In mostly all of the dark sector interacting theories, characterized by exchange rates $Q = 3H\xi f(\rho_c, \rho_x)$ (where f is an analytic function of the arguments ρ_c and/or ρ_x), the coupling parameter ξ is assumed to be independent of time (see however e.g. Ref. [54]). Unless one is interested in minimizing the number of extra parameters in the theory, there exists no underlying symmetry or law in nature which forbids such a dynamical coupling parameter. We have considered a very natural functional form for $\xi = \xi_0 + \xi_a(1 - a)$, that we have embedded into two possible interaction models, IVS1 ($Q = 3[\xi_0 + \xi_a(1 - a)]H\rho_x$) and IVS2 ($Q = 3[\xi_0 + \xi_a(1 - a)]H\frac{\rho_c\rho_x}{\rho_c + \rho_x}$).

We find that the interaction parameters ξ_0 and ξ_a , governing the dynamical behavior of the coupling ξ , are, in almost all cases, perfectly compatible with a non interacting scenario, showing a strong negative correlation among them. Nevertheless, for the CMB+R19 data combination, we find an indication for $\xi_a > 0$ at more than 2σ CL for IVS1. More importantly, when considering CMB data alone, we find, in general, that $\xi(z) > 0$, leading to a smaller value of the present matter density. In order to leave the CMB acoustic peaks location unchanged (which are mostly sensitive to the $\Omega_m h^2$ combination), a larger value of the Hubble constant H_0 is required. This in turn implies an optimal scenario where to address both the H_0 and S_8 tensions between early and late universe's observations.

Even if a Bayesian evidence analysis taking into account all observational datasets shows no particular preference for these interacting dark matter-dark energy models, a dynamical character in the interaction functions is still allowed by observations and can solve some pending issues related to high and low-redshift cosmological tensions.

Acknowledgments

The authors thank the referees for their important comments and suggestions aiming to improve the manuscript. WY acknowledges the support from the National Natural Science Foundation of China under Grants No. 11705079 and No. 11647153. OM is supported by the Spanish grants FPA2017-85985-P and SEV-2014-0398 of the MINECO and the European Union's Horizon 2020 research and innovation program

under the grant agreements No. 690575 and 674896. SP gratefully acknowledges several fruitful discussions with Prof. J. D. Barrow on this topic. The research of SP has been supported by the Mathematical Research Impact-Centric Support Scheme (MATRICS), File No. MTR/2018/000940, given by the Science and Engineer-

ing Research Board (SERB), Govt. of India, and also by the Faculty Research and Professional Development Fund (FRPDF) Scheme of Presidency University, Kolkata, India. EDV acknowledges support from the European Research Council in the form of a Consolidator Grant with number 681431.

-
- [1] N. Aghanim *et al.* [Planck Collaboration], *Planck 2018 results. VI. Cosmological parameters*, [arXiv:1807.06209 [astro-ph.CO]].
 - [2] N. Suzuki *et al.*, *The Hubble Space Telescope Cluster Supernova Survey: V. Improving the Dark Energy Constraints Above $z > 1$ and Building an Early-Type-Hosted Supernova Sample*, *Astrophys. J.* **746**, 85 (2012) [arXiv:1105.3470 [astro-ph.CO]].
 - [3] M. Crocce *et al.* [DES Collaboration], *Galaxy clustering, photometric redshifts and diagnosis of systematics in the DES Science Verification data*, *Mon. Not. Roy. Astron. Soc.* **455**, no.4, 4301 (2016) [arXiv:1507.05360 [astro-ph.CO]].
 - [4] S. Alam *et al.* [SDSS-III Collaboration], *The Eleventh and Twelfth Data Releases of the Sloan Digital Sky Survey: Final Data from SDSS-III*, *Astrophys. J. Suppl.* **219**, no.1, 12 (2015) [arXiv:1501.00963 [astro-ph.IM]].
 - [5] G. Hinshaw *et al.* [WMAP Collaboration], *Nine-Year Wilkinson Microwave Anisotropy Probe (WMAP) Observations: Cosmological Parameter Results*, *Astrophys. J. Suppl.* **208**, 19 (2013) [arXiv:1212.5226 [astro-ph.CO]].
 - [6] P. A. R. Ade *et al.* [Planck Collaboration], *Planck 2015 results. XIII. Cosmological parameters*, *Astron. Astrophys.* **594**, A13 (2016) [arXiv:1502.01589 [astro-ph.CO]].
 - [7] S. M. Carroll, *Quintessence and the rest of the world*, *Phys. Rev. Lett.* **81**, 3067 (1998) [astro-ph/9806099].
 - [8] C. Wetterich, *The Cosmon model for an asymptotically vanishing time dependent cosmological 'constant'*, *Astron. Astrophys.* **301**, 321 (1995) [hep-th/9408025].
 - [9] L. Amendola, *Coupled Quintessence*, *Phys. Rev. D* **62**, 043511 (2000) [arXiv:astro-ph/9908023].
 - [10] L. Amendola and C. Quercellini, *Tracking and coupled dark energy as seen by WMAP*, *Phys. Rev. D* **68**, 023514 (2003) [arXiv:astro-ph/0303228].
 - [11] D. Pavón and W. Zimdahl, *Holographic dark energy and cosmic coincidence*, *Phys. Lett. B* **628**, 206 (2005) [arXiv:gr-qc/0505020].
 - [12] S. del Campo, R. Herrera and D. Pavón, *Toward a solution of the coincidence problem*, *Phys. Rev. D* **78**, 021302 (2008) [arXiv:0806.2116 [astro-ph]].
 - [13] S. del Campo, R. Herrera and D. Pavón, *Interacting models may be key to solve the cosmic coincidence problem*, *J. Cosmol. Astropart. Phys.* **0901**, 020 (2009) [arXiv:0812.2210 [gr-qc]].
 - [14] S. Das, P. S. Corasaniti and J. Khoury, *Super-acceleration as signature of dark sector interaction*, *Phys. Rev. D* **73**, 083509 (2006) [astro-ph/0510628].
 - [15] H. M. Sadjadi and M. Honardoost, *Thermodynamics second law and $\omega = -1$ crossing(s) in interacting holographic dark energy model*, *Phys. Lett. B* **647**, 231 (2007) [gr-qc/0609076].
 - [16] S. Pan and S. Chakraborty, *A cosmographic analysis of holographic dark energy models*, *Int. J. Mod. Phys. D* **23**, no. 11, 1450092 (2014) [arXiv:1410.8281 [gr-qc]].
 - [17] A. P. Billyard and A. A. Coley, *Interactions in scalar field cosmology*, *Phys. Rev. D* **61**, 083503 (2000) [astro-ph/9908224].
 - [18] J. D. Barrow and T. Clifton, *Cosmologies with energy exchange*, *Phys. Rev. D* **73**, 103520 (2006) [gr-qc/0604063].
 - [19] L. Amendola, G. Camargo Campos and R. Rosenfeld, *Consequences of dark matter-dark energy interaction on cosmological parameters derived from SNIa data*, *Phys. Rev. D* **75**, 083506 (2007) [astro-ph/0610806].
 - [20] J. H. He and B. Wang, *Effects of the interaction between dark energy and dark matter on cosmological parameters*, *JCAP* **0806**, 010 (2008) [arXiv:0801.4233 [astro-ph]].
 - [21] J. Våliviita, E. Majerotto and R. Maartens, *Instability in interacting dark energy and dark matter fluids*, *JCAP* **0807**, 020 (2008) [arXiv:0804.0232 [astro-ph]].
 - [22] M. B. Gavela, D. Hernandez, L. Lopez Honorez, O. Mena and S. Rigolin, *Dark coupling*, *JCAP* **0907**, 034 (2009) [arXiv:0901.1611 [astro-ph.CO]].
 - [23] E. Majerotto, J. Valiviita and R. Maartens, *Adiabatic initial conditions for perturbations in interacting dark energy models*, *Mon. Not. Roy. Astron. Soc.* **402**, 2344 (2010) [arXiv:0907.4981 [astro-ph.CO]].
 - [24] M. B. Gavela, L. Lopez Honorez, O. Mena and S. Rigolin, *Dark Coupling and Gauge Invariance*, *JCAP* **1011**, 044 (2010) [arXiv:1005.0295 [astro-ph.CO]].
 - [25] T. Clemson, K. Koyama, G. B. Zhao, R. Maartens and J. Valiviita, *Interacting Dark Energy – constraints and degeneracies*, *Phys. Rev. D* **85**, 043007 (2012) [arXiv:1109.6234 [astro-ph.CO]].
 - [26] S. Pan, S. Bhattacharya and S. Chakraborty, *An analytic model for interacting dark energy and its observational constraints*, *Mon. Not. Roy. Astron. Soc.* **452**, no.3, 3038 (2015) [arXiv:1210.0396 [gr-qc]].
 - [27] S. Pan and S. Chakraborty, *Will there be again a transition from acceleration to deceleration in course of the dark energy evolution of the universe?*, *Eur. Phys. J. C* **73**, 2575 (2013) [arXiv:1303.5602 [gr-qc]].
 - [28] W. Yang and L. Xu, *Testing coupled dark energy with large scale structure observation*, *JCAP* **1408**, 034 (2014) [arXiv:1401.5177 [astro-ph.CO]].
 - [29] W. Yang and L. Xu, *Cosmological constraints on interacting dark energy with redshift-space distortion after Planck data*, *Phys. Rev. D* **89**, no.8, 083517 (2014) [arXiv:1401.1286 [astro-ph.CO]].
 - [30] S. Pan and G. S. Sharov, *A model with interaction of dark components and recent observational data*, *Mon. Not. Roy. Astron. Soc.* **472**, no. 4, 4736 (2017) [arXiv:1609.02287 [gr-qc]].
 - [31] A. Mukherjee and N. Banerjee, *In search of the dark matter dark energy interaction: a kinematic approach*, *Class. Quant. Grav.* **34**, no. 3, 035016 (2017) [arXiv:1610.04419 [astro-ph.CO]].

- [32] G. S. Sharov, S. Bhattacharya, S. Pan, R. C. Nunes and S. Chakraborty, *A new interacting two fluid model and its consequences*, Mon. Not. Roy. Astron. Soc. **466**, 3497 (2017) [arXiv:1701.00780 [gr-qc]].
- [33] W. Yang, N. Banerjee and S. Pan, *Constraining a dark matter and dark energy interaction scenario with a dynamical equation of state*, Phys. Rev. D **95**, no. 12, 123527 (2017) [arXiv:1705.09278 [astro-ph.CO]].
- [34] W. Yang, S. Pan and D. F. Mota, *Novel approach toward the large-scale stable interacting dark-energy models and their astronomical bounds*, Phys. Rev. D **96**, no. 12, 123508 (2017) [arXiv:1709.00006 [astro-ph.CO]].
- [35] S. Pan, A. Mukherjee and N. Banerjee, *Astronomical bounds on a cosmological model allowing a general interaction in the dark sector*, Mon. Not. Roy. Astron. Soc. **477**, 1189 (2018) [arXiv:1710.03725 [astro-ph.CO]].
- [36] W. Yang, S. Pan and A. Paliathanasis, *Cosmological constraints on an exponential interaction in the dark sector*, Mon. Not. Roy. Astron. Soc. **482**, no.1, 1007 (2019) [arXiv:1804.08558 [gr-qc]].
- [37] W. Yang, S. Pan, L. Xu and D. F. Mota, *Effects of anisotropic stress in interacting dark matter dark energy scenarios*, Mon. Not. Roy. Astron. Soc. **482**, no. 2, 1858 (2019) [arXiv:1804.08455 [astro-ph.CO]].
- [38] W. Yang, S. Pan, R. Herrera and S. Chakraborty, *Large-scale (in) stability analysis of an exactly solved coupled dark-energy model*, Phys. Rev. D **98**, no.4, 043517 (2018) [arXiv:1808.01669 [gr-qc]].
- [39] M. Martinelli, N. B. Hogg, S. Peirone, M. Bruni and D. Wands, *Constraints on the interacting vacuum - geodesic CDM scenario*, arXiv:1902.10694 [astro-ph.CO].
- [40] A. Paliathanasis, S. Pan and W. Yang, *Dynamics of non-linear interacting dark energy models*, arXiv:1903.02370 [gr-qc].
- [41] S. Pan, W. Yang, C. Singha and E. N. Saridakis, *Observational constraints on sign-changeable interaction models and alleviation of the H_0 tension*, arXiv:1903.10969 [astro-ph.CO].
- [42] W. Yang, S. Pan, E. Di Valentino, B. Wang and A. Wang, *Forecasting Interacting Vacuum-Energy Models using Gravitational Waves*, arXiv:1904.11980 [astro-ph.CO].
- [43] W. Yang, S. Vagnozzi, E. Di Valentino, R. C. Nunes, S. Pan and D. F. Mota, *Listening to the sound of dark sector interactions with gravitational wave standard sirens*, arXiv:1905.08286 [astro-ph.CO].
- [44] S. Kumar and R. C. Nunes, *Echo of interactions in the dark sector*, Phys. Rev. D **96**, no. 10, 103511 (2017) [arXiv:1702.02143 [astro-ph.CO]].
- [45] E. Di Valentino, A. Melchiorri and O. Mena, *Can interacting dark energy solve the H_0 tension?*, Phys. Rev. D **96**, no. 4, 043503 (2017) [arXiv:1704.08342 [astro-ph.CO]].
- [46] W. Yang, S. Pan, E. Di Valentino, R. C. Nunes, S. Vagnozzi and D. F. Mota, *Tale of stable interacting dark energy, observational signatures, and the H_0 tension*, JCAP **1809**, 019, (2018) [arXiv:1805.08252 [astro-ph.CO]].
- [47] W. Yang, A. Mukherjee, E. Di Valentino and S. Pan, *Interacting dark energy with time varying equation of state and the H_0 tension*, Phys. Rev. D **98**, no. 12, 123527 (2018) [arXiv:1809.06883 [astro-ph.CO]].
- [48] V. Salvatelli, N. Said, M. Bruni, A. Melchiorri and D. Wands, *Indications of a late-time interaction in the dark sector*, Phys. Rev. Lett. **113**, no. 18, 181301 (2014) [arXiv:1406.7297 [astro-ph.CO]].
- [49] R. C. Nunes, S. Pan and E. N. Saridakis, *New constraints on interacting dark energy from cosmic chronometers*, Phys. Rev. D **94**, 023508 (2016) [arXiv:1605.01712 [astro-ph.CO]].
- [50] S. Kumar and R. C. Nunes, *Probing the interaction between dark matter and dark energy in the presence of massive neutrinos*, Phys. Rev. D **94**, 123511 (2016) [arXiv:1608.02454 [astro-ph.CO]].
- [51] C. van de Bruck, J. Mifsud and J. Morrice, *Testing coupled dark energy models with their cosmological background evolution*, Phys. Rev. D **95**, no. 4, 043513 (2017) [arXiv:1609.09855 [astro-ph.CO]].
- [52] W. Yang, H. Li, Y. Wu and J. Lu, *Cosmological constraints on coupled dark energy*, JCAP **1610**, no.10, 007 (2016) [arXiv:1608.07039 [astro-ph.CO]].
- [53] W. Yang, S. Pan and J. D. Barrow, *Large-scale Stability and Astronomical Constraints for Coupled Dark-Energy Models*, Phys. Rev. D **97**, no. 4, 043529 (2018) [arXiv:1706.04953 [astro-ph.CO]].
- [54] Y. Wang and G. B. Zhao, *Constraining the dark matter-vacuum energy interaction using the EDGES 21-cm absorption signal*, Astrophys. J. **869**, no. 1, 26 (2018) [arXiv:1805.11210 [astro-ph.CO]].
- [55] V. F. Mukhanov, H. A. Feldman and R. H. Brandenberger, *Theory of cosmological perturbations*, Phys. Rept. **215**, 203 (1992).
- [56] C. P. Ma and E. Bertschinger, *Cosmological perturbation theory in the synchronous and conformal Newtonian gauges*, Astrophys. J. **455**, 7 (1995) [arXiv:astro-ph/9506072].
- [57] K. A. Malik and D. Wands, *Cosmological perturbations*, Phys. Rept. **475**, 1 (2009) [arXiv:0809.4944 [astro-ph]].
- [58] Y. Wang, D. Wands, G. B. Zhao and L. Xu, *Post-Planck constraints on interacting vacuum energy*, Phys. Rev. D **90**, no. 2, 023502 (2014) [arXiv:1404.5706 [astro-ph.CO]].
- [59] Y. H. Li and X. Zhang, *Running coupling: Does the coupling between dark energy and dark matter change sign during the cosmological evolution?*, Eur. Phys. J. C **71**, 1700 (2011) [arXiv:1103.3185 [astro-ph.CO]].
- [60] J. J. Guo, J. F. Zhang, Y. H. Li, D. Z. He and X. Zhang, *Probing the sign-changeable interaction between dark energy and dark matter with current observations*, Sci. China Phys. Mech. Astron. **61**, no. 3, 030011 (2018) [arXiv:1710.03068 [astro-ph.CO]].
- [61] A. Shafieloo, D. K. Hazra, V. Sahni and A. A. Starobinsky, *Metastable Dark Energy with Radioactive-like Decay*, Mon. Not. Roy. Astron. Soc. **473**, no. 2, 2760 (2018) [arXiv:1610.05192 [astro-ph.CO]].
- [62] R. G. Landim and E. Abdalla, *Metastable dark energy*, Phys. Lett. B **764**, 271 (2017) [arXiv:1611.00428 [hep-ph]].
- [63] M. Szydlowski, A. Stachowski and K. Urbanowski, *Quantum mechanical look at the radioactive-like decay of metastable dark energy*, Eur. Phys. J. C **77**, no. 12, 902 (2017) [arXiv:1704.05364 [gr-qc]].
- [64] X. L. Li, A. Shafieloo, V. Sahni and A. A. Starobinsky, *Revisiting Metastable Dark Energy and Tensions in the Estimation of Cosmological Parameters*, arXiv:1904.03790 [astro-ph.CO].
- [65] R. Adam et al. [Planck Collaboration], *Planck 2015 results. I. Overview of products and scientific results*, Astron. Astrophys. **594**, A1 (2016) [arXiv:1502.01582

- [astro-ph.CO]].
- [66] N. Aghanim *et al.* [Planck Collaboration], *Planck 2015 results. XI. CMB power spectra, likelihoods, and robustness of parameters*, *Astron. Astrophys.* **594**, A11 (2016) [arXiv:1507.02704 [astro-ph.CO]].
- [67] F. Beutler *et al.*, *The 6dF Galaxy Survey: Baryon Acoustic Oscillations and the Local Hubble Constant*, *Mon. Not. Roy. Astron. Soc.* **416**, 3017 (2011) [arXiv:1106.3366 [astro-ph.CO]].
- [68] A. J. Ross, L. Samushia, C. Howlett, W. J. Percival, A. Burden and M. Manera, *The clustering of the SDSS DR7 main Galaxy sample - I. A 4 per cent distance measure at $z = 0.15$* , *Mon. Not. Roy. Astron. Soc.* **449**, no. 1, 835 (2015) [arXiv:1409.3242 [astro-ph.CO]].
- [69] H. Gil-Marín *et al.*, *The clustering of galaxies in the SDSS-III Baryon Oscillation Spectroscopic Survey: BAO measurement from the LOS-dependent power spectrum of DR12 BOSS galaxies*, *Mon. Not. Roy. Astron. Soc.* **460**, no. 4, 4210 (2016) [arXiv:1509.06373 [astro-ph.CO]].
- [70] D. M. Scolnic *et al.*, *The Complete Light-curve Sample of Spectroscopically Confirmed SNe Ia from Pan-STARRS1 and Cosmological Constraints from the Combined Pantheon Sample*, *Astrophys. J.* **859**, no. 2, 101 (2018) [arXiv:1710.00845 [astro-ph.CO]].
- [71] A. G. Riess, S. Casertano, W. Yuan, L. M. Macri and D. Scolnic, *Large Magellanic Cloud Cepheid Standards Provide a 1% Foundation for the Determination of the Hubble Constant and Stronger Evidence for Physics Beyond Λ CDM*, [arXiv:1903.07603 [astro-ph.CO]].
- [72] A. Lewis and S. Bridle, *Cosmological parameters from CMB and other data: A Monte Carlo approach*, *Phys. Rev. D* **66**, 103511 (2002) [astro-ph/0205436].
- [73] A. Lewis, A. Challinor and A. Lasenby, *Efficient computation of CMB anisotropies in closed FRW models*, *Astrophys. J.* **538**, 473 (2000) [astro-ph/9911177].
- [74] E. Di Valentino and S. Bridle, *Exploring the Tension between Current Cosmic Microwave Background and Cosmic Shear Data*, *Symmetry* **10**, no. 11, 585 (2018).
- [75] K. Kuijken *et al.*, *Gravitational Lensing Analysis of the Kilo Degree Survey*, *Mon. Not. Roy. Astron. Soc.* **454**, no. 4, 3500 (2015) [arXiv:1507.00738 [astro-ph.CO]].
- [76] H. Hildebrandt *et al.*, *KiDS-450: Cosmological parameter constraints from tomographic weak gravitational lensing*, *Mon. Not. Roy. Astron. Soc.* **465**, 1454 (2017) [arXiv:1606.05338 [astro-ph.CO]].
- [77] I. Fenech Conti, R. Herbonnet, H. Hoekstra, J. Merten, L. Miller and M. Viola, *Calibration of weak-lensing shear in the Kilo-Degree Survey*, *Mon. Not. Roy. Astron. Soc.* **467**, no. 2, 1627 (2017) [arXiv:1606.05337 [astro-ph.CO]].
- [78] T. M. C. Abbott *et al.* [DES Collaboration], *Dark Energy Survey year 1 results: Cosmological constraints from galaxy clustering and weak lensing*, *Phys. Rev. D* **98**, no. 4, 043526 (2018) [arXiv:1708.01530 [astro-ph.CO]].
- [79] M. A. Troxel *et al.* [DES Collaboration], *Dark Energy Survey Year 1 results: Cosmological constraints from cosmic shear*, *Phys. Rev. D* **98**, no. 4, 043528 (2018) [arXiv:1708.01538 [astro-ph.CO]].
- [80] C. Heymans *et al.*, *CFHTLenS: The Canada-France-Hawaii Telescope Lensing Survey*, *Mon. Not. Roy. Astron. Soc.* **427**, 146 (2012) [arXiv:1210.0032 [astro-ph.CO]].
- [81] T. Erben *et al.*, *CFHTLenS: The Canada-France-Hawaii Telescope Lensing Survey - Imaging Data and Catalogue Products*, *Mon. Not. Roy. Astron. Soc.* **433**, 2545 (2013) [arXiv:1210.8156 [astro-ph.CO]].
- [82] S. Joudaki *et al.*, *CFHTLenS revisited: assessing concordance with Planck including astrophysical systematics*, *Mon. Not. Roy. Astron. Soc.* **465**, no. 2, 2033 (2017) [arXiv:1601.05786 [astro-ph.CO]].
- [83] X. Zhang and Q. G. Huang, *Constraints on H_0 from WMAP and BAO Measurements*, *Commun. Theor. Phys.* **71**, no. 7, 826 (2019) [arXiv:1812.01877 [astro-ph.CO]].
- [84] W. Yang, S. Pan, E. Di Valentino, E. N. Saridakis and S. Chakraborty, *Observational constraints on one-parameter dynamical dark-energy parametrizations and the H_0 tension*, *Phys. Rev. D* **99**, no. 4, 043543 (2019) [arXiv:1810.05141 [astro-ph.CO]].
- [85] A. Heavens, Y. Fantaye, A. Mootoovaloo, H. Eggers, Z. Hosenie, S. Kroon and E. Sellentin, *Marginal Likelihoods from Monte Carlo Markov Chains*, [arXiv:1704.03472 [stat.CO]].
- [86] A. Heavens, Y. Fantaye, E. Sellentin, H. Eggers, Z. Hosenie, S. Kroon and A. Mootoovaloo, *No evidence for extensions to the standard cosmological model*, *Phys. Rev. Lett.* **119**, no. 10, 101301 (2017). [arXiv:1704.03467 [astro-ph.CO]].
- [87] S. Pan, E. N. Saridakis and W. Yang, *Observational Constraints on Oscillating Dark-Energy Parametrizations*, *Phys. Rev. D* **98**, no. 6, 063510 (2018) [arXiv:1712.05746 [astro-ph.CO]].
- [88] R. E. Kass and A. E. Raftery, *Bayes factors*, *J. Am. Statist. Assoc.* **90**, no.430, 773 (1995).